JVI Journals.ASM.org

Latent Expression of the Epstein-Barr Virus (EBV)-Encoded Major Histocompatibility Complex Class I TAP Inhibitor, *BNLF2a*, in EBV-Positive Gastric Carcinomas

Michael J. Strong,[a,b] Thomas Laskow,[a,b] Hani Nakhoul,[a,b] Eugene Blanchard,[c] Yaozhong Liu,[d] Xia Wang,[a] Melody Baddoo,[a,b] Zhen Lin,[a,b] Qinyan Yin,[b,e] Erik K. Flemington[a,b]

Department of Pathology, Tulane University Health Sciences Center, New Orleans, Louisiana, USA[a]; Tulane Cancer Center, New Orleans, Louisiana, USA[b]; Department of Microbiology, Immunology & Parasitology, Louisiana State University School of Medicine, New Orleans, Louisiana, USA[c]; Department of Biostatistics and Bioinformatics, Tulane University Health Sciences Center, New Orleans, Louisiana, USA[d]; Department of Pulmonary Diseases, Critical Care, and Environmental Medicine, Tulane University Health Sciences Center, New Orleans, Louisiana, USA[e]

The Epstein-Barr virus (EBV) *BNLF2a* gene product provides immune evasion properties to infected cells through inhibition of transporter associated with antigen processing (TAP)-mediated transport of antigen peptides. Although *BNLF2a* is considered to be a lytic gene, we demonstrate that it is expressed in nearly half of the EBV-associated gastric carcinomas analyzed. Further, we show that *BNLF2a* expression is dissociated from lytic gene expression. *BNLF2a* is therefore expressed in this latency setting, potentially helping protect the infected tumor cells from immunosurveillance.

The early lytic gene *BNLF2a* plays an integral role in evading immune recognition of Epstein-Barr virus (EBV)-infected cells undergoing lytic replication, a setting where substantial numbers of viral antigens are expressed (1–7). BNLF2a functions through inhibition of peptide loading onto major histocompatibility complex (MHC) class I molecules, thereby blocking antigen presentation to cytotoxic T lymphocytes (2–7). In contrast to the lytic phase of the EBV infection cycle, latent infection typically results in a highly restricted pattern of gene expression where primarily noncoding RNAs and a minimal number of viral protein-coding genes are expressed, presumably lessening the dependence on overt adaptive immune inhibitory mechanisms.

We previously found one of the four EBV-positive gastric carcinoma (GC) biopsy specimens from an early The Cancer Genome Atlas (TCGA) gastric adenocarcinoma cohort that unexpectedly showed expression of the viral lytic immune evasion gene *BNLF2a* (1). We raised the possibility that though the finding of only a single *BNLF2a*-positive sample may be incidental, its expression in gastric cancer could be a means of providing antitumor and/or antivirus immune responses (1).

To investigate this issue further, we first performed a global virome analysis on the expanded cohort of patient GC RNA-seq ($n = 285$) and whole-exome sequence (WXS) ($n = 352$) data sets from TCGA (8), using a directed virome analysis approach that we have reported previously (9, 10). For this analysis, all RNA-seq and WXS data sets were aligned to an index containing the human genome (Genome Reference Consortium GRCh37) plus 740 mammalian viral genomes, using the transcript aligner STAR (Spliced Transcripts Alignment to a Reference) (11) run with default options plus the clip5pNbases 6 and outFilterMultimapNmax 1000 command options (removes the first 6 bases of each read and filters out any reads that map to more than 1,000 regions of the genome, respectively). As a way to help gauge true tumor virus association from systemic viral infection, we analyzed 33 RNA-seq TCGA data sets from matched normal gastric tissues. We also performed a virome analysis on 23 RNA-seq gastric cancer cell line data sets from the Cancer Cell Line Encyclopedia (CCLE) project (12).

No substantial viral reads were detected in any of the normal gastric RNA-seq data sets (Fig. 1A; see also Table S1 in the supplemental material). In line with TCGA marker paper (8), we identified 25 GC biopsy specimens with substantial EBV reads in both the RNA-seq and the WXS data (Fig. 1A), although lower EBV read numbers were observed in some additional samples (14 RNA-seq data sets and 11 WXS data sets) that possibly represent low-level infections or the presence of EBV-positive infiltrating B cells (see Tables S1 and S2 in the supplemental material). We also detected human cytomegalovirus (HCMV) reads in 19 RNA-seq and 6 WXS samples (Fig. 1A; see also Tables S1 and S2 in the supplemental material). Although HCMV read numbers were low in most cases, they were detected in both the RNA-seq data and the WGS data in two cases, raising the possibility of low-level infections. Of the GC cell line RNA-seq data sets analyzed, the SNU719 cell line was the only one in which EBV was detected (Fig. 1B). Notably, very high murine leukemia virus (MuLV) read levels (1.5% of human mapped reads) were detected in the LMSU cell line (Fig. 1B; see also Table S3 in the supplemental material), which likely reflects incidental laboratory infection of this cell line, similar to previous MuLV virome findings from our lab for other cell lines (9, 13).

Analysis of read coverage across the EBV genome for all EBV-

Received 30 April 2015 **Accepted** 7 July 2015

Accepted manuscript posted online 15 July 2015

Citation Strong MJ, Laskow T, Nakhoul H, Blanchard E, Liu Y, Wang X, Baddoo M, Lin Z, Yin Q, Flemington EK. 2015. Latent expression of the Epstein-Barr virus (EBV)-encoded major histocompatibility complex class I TAP inhibitor, *BNLF2a*, in EBV-positive gastric carcinomas. J Virol 89:10110–10114. doi:10.1128/JVI.01110-15.

Editor: R. M. Longnecker

Address correspondence to Erik K. Flemington, erik@tulane.edu.

Supplemental material for this article may be found at http://dx.doi.org/10.1128/JVI.01110-15.

doi:10.1128/JVI.01110-15

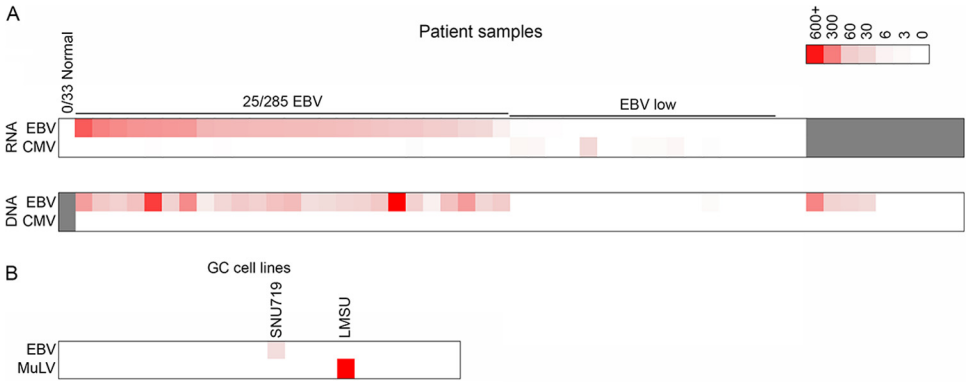

FIG 1 Heat map showing the number of viral reads per million human mapped reads for the TCGA GC patient biopsy specimens (A) and for the 23 GC cell lines (B). Viruses included in this display are those showing at least 2 viral reads per million human mapped reads in at least one RNA-seq sample.

positive TCGA GC samples with high EBV read numbers showed the expected high-level expression of the noncoding *RPMS1* transcript region (see Fig. S1 in the supplemental material) (8), low-level expression of *EBNA1*, and low-level expression of the immediate early and early genes *BZLF1*, *BSLF2/BMLF1*, and *BMRF1*, which were inconsistently expressed across samples (data not shown). Also consistent with previous studies (1, 8), expression of the latent membrane protein 2 (*LMP2*) gene was detected in most samples (see Fig. S2 in the supplemental material). In addition to these regions, however, we observed good read coverage across the *BNLF2a* locus in about half of the samples (Fig. 2), suggesting that *BNLF2a* is, in fact, expressed in a substantial proportion of EBV-associated GCs.

Since the TCGA RNA-seq data were generated using library preparation protocols that do not retain source strand information, we sought to investigate the orientation of read coverage at the *BNLF2a* region in GC biopsy specimens. We analyzed RNAs from 18 independent gastric cancer biopsy specimens (Bioserve) for the presence of EBV through quantitative reverse transcriptase PCR (qRT-PCR) analysis for *EBER1* and *RPMS1* expression. Two samples were found to be EBV positive (1). RNAs from these samples were subjected to ribodepletion (Ribo-Zero, catalog no. MRZH11124; Epicentre) and the generation of strand-specific TruSeq (catalog no. RS-930-2001; Illumina) sequencing libraries. The libraries were sequenced on an Illumina HiSeq 2000 machine and aligned to the Akata EBV genome (14). One of these samples, WZQ1TALM, showed good coverage at the *BNLF2a* locus, and reads were found to derive from leftward transcripts (Fig. 2), consistent with the expression of the leftward-oriented *BNLF2a* gene.

To confirm that *BNLF2a* can be expressed from tumor cells rather than potentially from EBV-infected stromal components, we performed strand-specific sequencing of three known EBV-positive gastric carcinoma cell lines, SNU719, NCC24, and YCCEL-1 (15–17). SNU719 and YCCEL-1 showed good leftward coverage at the *BNLF2a* locus (Fig. 2), demonstrating the expression of *BNLF2a* in GC tumor cells. Further, both SNU719 and YCCEL-1, but not NCC24 or EBV-negative AGS cells, were found to express BNLF2a protein at levels comparable to that observed in the Burkitt's lymphoma cell line Akata, which was induced to undergo reactivation (Fig. 3).

Since *BNLF2a* is an early lytic gene, we next assessed whether *BNLF2a* expression was linked to EBV reactivation, due either to full lytic replication in a fraction of cells or to cells exhibiting abortive lytic replication. First, for each of the 25 EBV-positive TCGA GC samples, we calculated the ratio of *BNLF2a* read numbers to the total number of reads derived from all lytic genes (excluding reads corresponding to lytic genes that overlap with the *RPMS1* gene and reads mapping to the *BHLF1* locus, whose expression can be decoupled from reactivation in some settings). First, it is notable that *BNLF2a* reads make up the majority of the analyzed lytic reads in four samples and generally comprise a substantial proportion of lytic reads in more than half of the samples (Fig. 4A). This is in contrast to the ratio of *BNLF2a* reads observed during reactivation of Akata cells, where the proportion of *BNLF2a* reads is 0.006 (Fig. 4A). Second, the *BNLF2a* read numbers do not appear to correspond to the proportion of lytic reads that map to the immediate early *BZLF1* gene (Fig. 4A).

To more accurately assess the relationship between *BNLF2a* and *BZLF1* expression across samples, we determined the correlation coefficient between *BNLF2a* and *BZLF1* expression. For this analysis, we calculated the number of *BNLF2a* and *BZLF1* reads per million reads mapping to the human or EBV genome for each sample. These values were then plotted in a scatter plot, and the correlation coefficient was calculated. This analysis showed no correlation between *BNLF2a* expression and *BZLF1* (Fig. 4B). Similarly, no correlation was observed between *BNLF2a* and the early gene *BSLF2/BMLF1* (Fig. 4B). In contrast, the correlation coefficient between *BZLF1* and *BSLF2/BMLF1* was found to be 0.75 (Fig. 4B). Although there are only very low read numbers mapping to the *LMP1* gene outside of the region that overlaps with *BNLF2a*, we assessed whether there was any correlation between the levels of *BNLF2a* and *LMP1*. Little correlation was observed between *BNLF2a* and *LMP1* (Fig. 4B). Taken together, these results indicate that *BNLF2a* expression is decoupled from reactivation in GCs, indicating that its expression is instead controlled by potential tissue-specific cellular factors and/or epigenetic marks in this setting.

Since the lytic gene *BHLF1* has similarly been shown to exhibit lytic cycle-independent expression in some cases, we calculated the correlation coefficients between *BHLF1* and *BNLF2a*, between *BHLF1* and *BZLF1*, and between *BHLF1* and *BSLF2/BMLF1*. The correlation coefficients for these relationships were found to be 0.46, 0.3, and 0.6, respectively. While some samples showed expression of both *BHLF1* and *BNLF2a*, the correlation between *BHLF1* and *BNLF2a* expression is low, and expression of *BNLF2a*

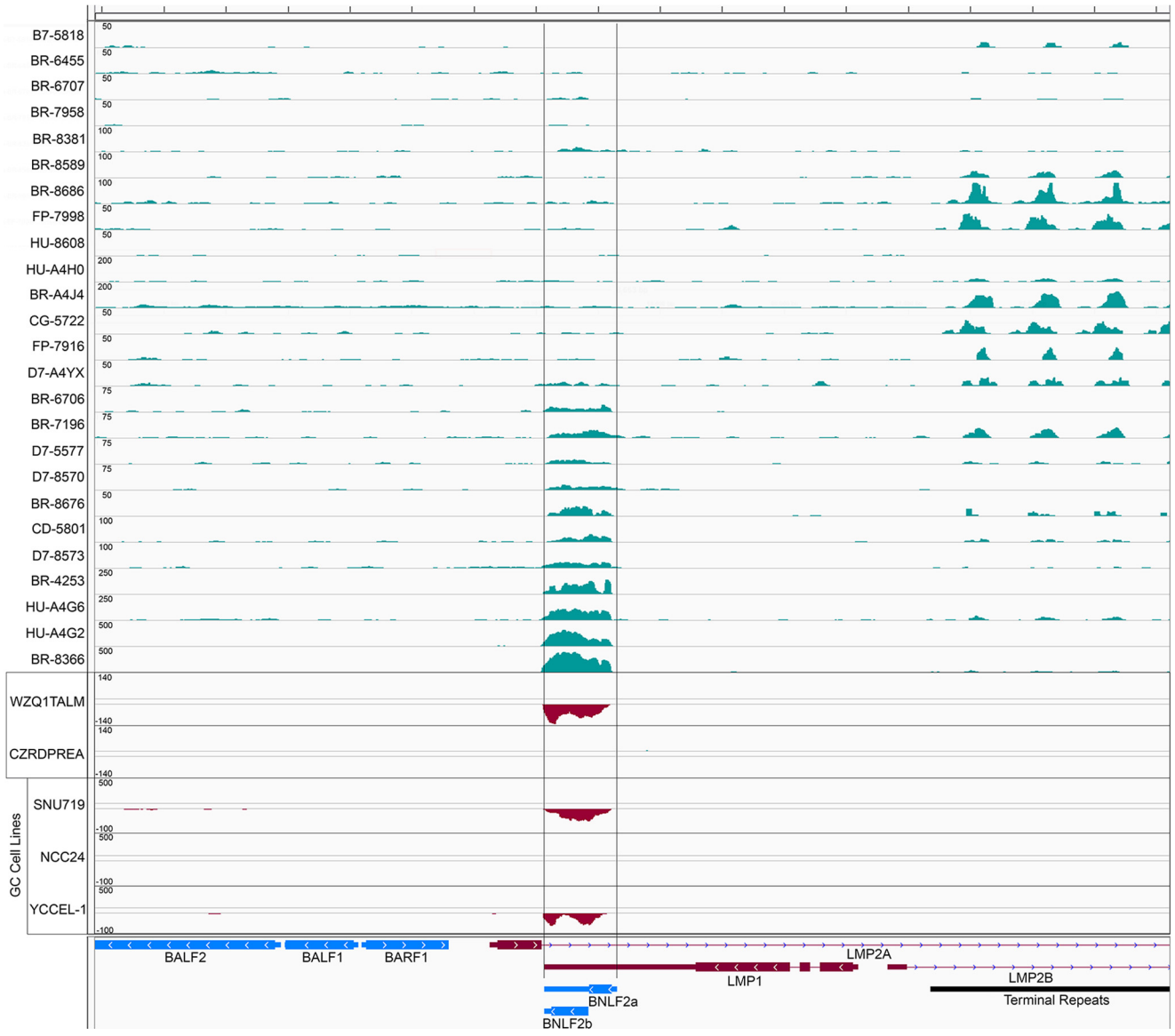

FIG 2 Genome browser view of the *BNLF2a* locus for 25 EBV-positive TCGA GC biopsy specimens, two additional EBV-positive GC tumor biopsy specimens sequenced using the stranded TruSeq library preparation protocol, and three EBV-positive GC cell lines sequenced using the stranded TruSeq library preparation protocol. Values on the *y* axis represent the number of reads spanning each genomic position. For the stranded sequencing reactions, sense strand coverage is indicated by positive *y* axis values and antisense strand coverage is indicated by negative *y* axis values.

is clearly observed in the absence of *BHLF1*. This indicates that although we cannot rule out some level of regulatory overlap with *BHLF1*, *BNLF2a*-specific mechanisms exist to drive its expression.

Many of the EBV genes known to be expressed in GCs, including the noncoding BamHI A rightward transcripts, the EBV-encoded microRNAs, the Pol III transcripts, *EBER1* and *EBER2*, and *LMP2*, likely contribute to oncogenesis through known influences on cell cycle and apoptosis pathways. Nevertheless, escape from immune surveillance is coming to be appreciated as one of the most critical steps in the development of cancer.

The finding that the lytic *BNLF2a* gene is expressed in gastric cancers independently of reactivation is important because it identifies a new form of type II latency (which we refer to as type

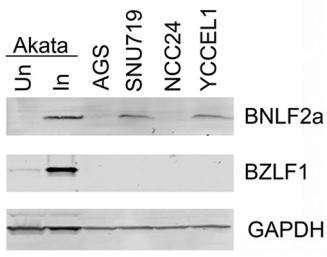

FIG 3 Western blot of *BNLF2a* expression in untreated Akata cells (Un), Akata cells treated with anti-human IgG for 24 h (In), the EBV-negative gastric cancer cell line AGS, and the EBV-positive gastric cell lines SNU719, NCC24, and YCCEL1. BNLF2a, BZLF1, and GAPDH were detected using the rat anti-BNLF2a monoclonal antibody 5F8 (a generous gift from Elizabeth Kremmer), a mouse anti-ZEBRA monoclonal antibody (catalog no. sc-53904; Santa Cruz Biotechnology), and a goat anti-GAPDH polyclonal antibody (catalog no. GTX100118; GeneTex), respectively.

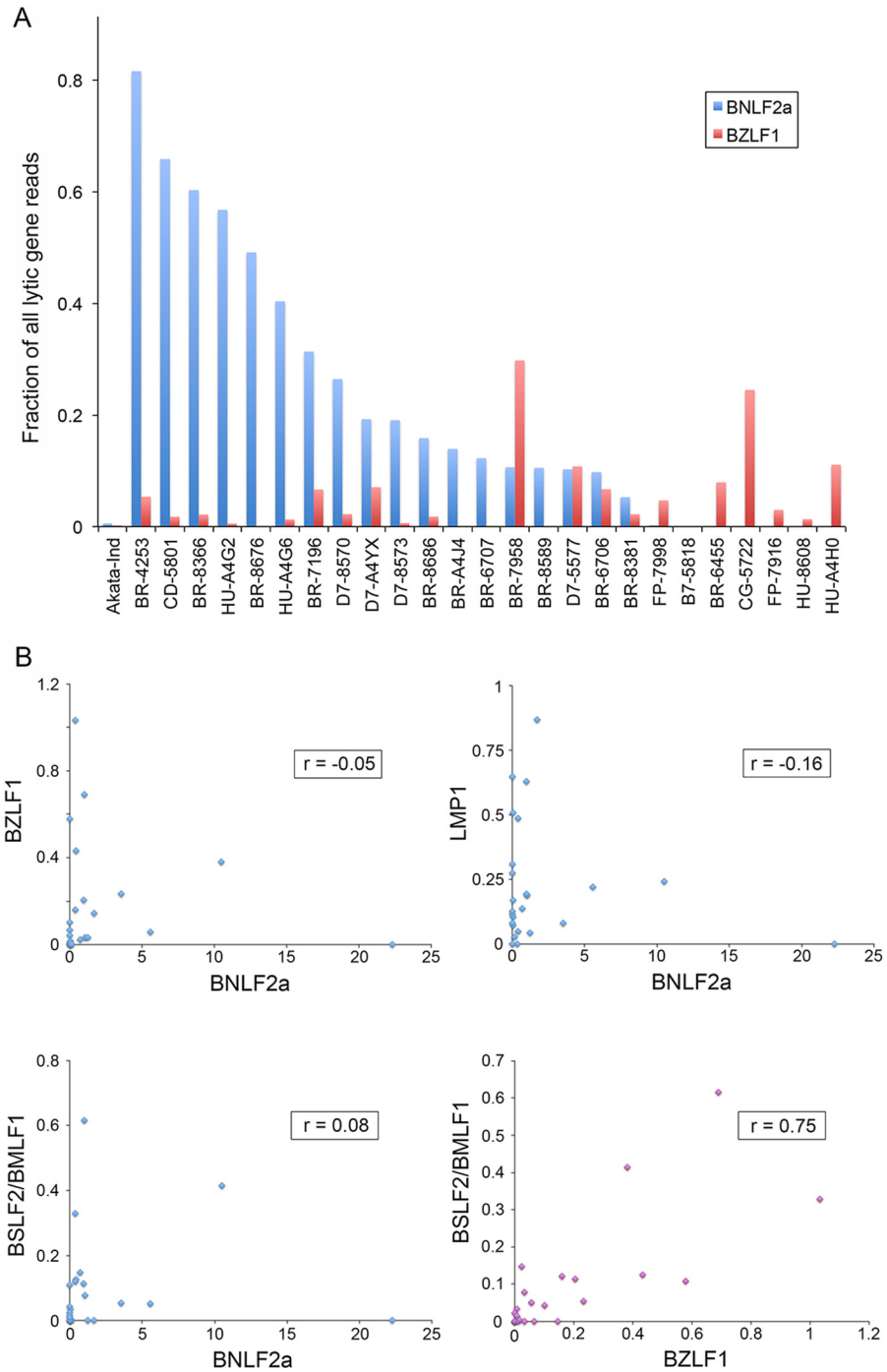

FIG 4 Expression of *BNLF2a* is uncoupled from lytic gene expression. (A) Fraction of lytic gene reads (sans *BHLF1* and lytic genes overlapping the *RPMS1* latency gene) that map to the *BNLF2a* and *BZLF1* genes for the 25 EBV-positive TCGA GC patient biopsy specimens and reactivated Akata cells (Akata-Ind) as a comparator. (B) Scatter plots and correlation coefficients calculated using normalized read counts for each of the indicated genes.

IIc, a latency program displaying expression of the protein-coding genes *EBNA1*, *LMP2*, and *BNLF2a*) and shows for the first time that EBV may contribute to GC survival and persistence through an immune evasion mechanism.

Microarray data accession numbers. Sequencing data is available from the NCBI GEO database under accession numbers GSE45453 and GSE70513.

ACKNOWLEDGMENTS

This study was supported by National Institutes of Health grants R01AI101046 and R01AI106676 to E.K.F., F30CA177267 to M.J.S., and P20GM103518 to Prescott Deininger, which supported the Tulane Cancer Center Next Generation Sequence Analysis Core, and a Louisiana Clinical and Translational Science Center pilot grant to Z.L.

Next-generation sequencing was performed at the University of Wis-

consin Biotechnology Center. Data analysis was carried out in the Tulane Cancer Center Next Generation Sequence Analysis Core using core computational resources. We thank Elizabeth Kremmer for graciously providing the 5F8 anti-BNLF2a antibody.

REFERENCES

1. **Strong MJ, Xu G, Coco J, Baribault C, Vinay DS, Lacey MR, Strong AL, Lehman TA, Seddon MB, Lin Z, Concha M, Baddoo M, Ferris M, Swan KF, Sullivan DE, Burow ME, Taylor CM, Flemington EK.** 2013. Differences in gastric carcinoma microenvironment stratify according to EBV infection intensity: implications for possible immune adjuvant therapy. PLoS Pathog **9:**e1003341. http://dx.doi.org/10.1371/journal.ppat.1003341.
2. **Bell MJ, Abbott RJ, Croft NP, Hislop AD, Burrows SR.** 2009. An HLA-A2-restricted T-cell epitope mapped to the BNLF2a immune evasion protein of Epstein-Barr virus that inhibits TAP. J Virol **83:**2783–2788. http://dx.doi.org/10.1128/JVI.01724-08.
3. **Horst D, van Leeuwen D, Croft NP, Garstka MA, Hislop AD, Kremmer E, Rickinson AB, Wiertz EJ, Ressing ME.** 2009. Specific targeting of the EBV lytic phase protein BNLF2a to the transporter associated with antigen processing results in impairment of HLA class I-restricted antigen presentation. J Immunol **182:**2313–2324. http://dx.doi.org/10.4049/jimmunol.0803218.
4. **Croft NP, Shannon-Lowe C, Bell AI, Horst D, Kremmer E, Ressing ME, Wiertz EJ, Middeldorp JM, Rowe M, Rickinson AB, Hislop AD.** 2009. Stage-specific inhibition of MHC class I presentation by the Epstein-Barr virus BNLF2a protein during virus lytic cycle. PLoS Pathog **5:**e1000490. http://dx.doi.org/10.1371/journal.ppat.1000490.
5. **Horst D, Favaloro V, Vilardi F, van Leeuwen HC, Garstka MA, Hislop AD, Rabu C, Kremmer E, Rickinson AB, High S, Dobberstein B, Ressing ME, Wiertz EJ.** 2011. EBV protein BNLF2a exploits host tail-anchored protein integration machinery to inhibit TAP. J Immunol **186:**3594–3605. http://dx.doi.org/10.4049/jimmunol.1002656.
6. **Wycisk AI, Lin J, Loch S, Hobohm K, Funke J, Wieneke R, Koch J, Skach WR, Mayerhofer PU, Tampe R.** 2011. Epstein-Barr viral BNLF2a protein hijacks the tail-anchored protein insertion machinery to block antigen processing by the transport complex TAP. J Biol Chem **286:**41402–41412. http://dx.doi.org/10.1074/jbc.M111.237784.
7. **Hislop AD, Ressing ME, van Leeuwen D, Pudney VA, Horst D, Koppers-Lalic D, Croft NP, Neefjes JJ, Rickinson AB, Wiertz EJ.** 2007. A CD8+ T cell immune evasion protein specific to Epstein-Barr virus and its close relatives in Old World primates. J Exp Med **204:**1863–1873. http://dx.doi.org/10.1084/jem.20070256.
8. **The Cancer Genome Atlas Research Network.** 2014. Comprehensive molecular characterization of gastric adenocarcinoma. Nature **513:**202–209. http://dx.doi.org/10.1038/nature13480.
9. **Cao S, Strong MJ, Wang X, Moss WN, Concha M, Lin Z, O'Grady T, Baddoo M, Fewell C, Renne R, Flemington EK.** 2015. High-throughput RNA sequencing-based virome analysis of 50 lymphoma cell lines from the Cancer Cell Line Encyclopedia project. J Virol **89:**713–729. http://dx.doi.org/10.1128/JVI.02570-14.
10. **Strong MJ, Baddoo M, Nanbo A, Xu M, Puetter A, Lin Z.** 2014. Comprehensive high-throughput RNA sequencing analysis reveals contamination of multiple nasopharyngeal carcinoma cell lines with HeLa cell genomes. J Virol **88:**10696–10704. http://dx.doi.org/10.1128/JVI.01457-14.
11. **Dobin A, Davis CA, Schlesinger F, Drenkow J, Zaleski C, Jha S, Batut P, Chaisson M, Gingeras TR.** 2013. STAR: ultrafast universal RNA-seq aligner. Bioinformatics **29:**15–21. http://dx.doi.org/10.1093/bioinformatics/bts635.
12. **Barretina J, Caponigro G, Stransky N, Venkatesan K, Margolin AA, Kim S, Wilson CJ, Lehar J, Kryukov GV, Sonkin D, Reddy A, Liu M, Murray L, Berger MF, Monahan JE, Morais P, Meltzer J, Korejwa A, Jane-Valbuena J, Mapa FA, Thibault J, Bric-Furlong E, Raman P, Shipway A, Engels IH, Cheng J, Yu GK, Yu J, Aspesi P, de Silva M, Jagtap K, Jones MD, Wang L, Hatton C, Palescandolo E, Gupta S, Mahan S, Sougnez C, Onofrio RC, Liefeld T, MacConaill L, Winckler W, Reich M, Li N, Mesirov JP, Gabriel SB, Getz G, Ardlie K, Chan V, Myer VE, Weber BL, Porter J, Warmuth M, Finan P, Harris JL, Meyerson M, Golub TR, Morrissey MP, Sellers WR, Schlegel R, Garraway LA.** 2012. The Cancer Cell Line Encyclopedia enables predictive modelling of anticancer drug sensitivity. Nature **483:**603–607. http://dx.doi.org/10.1038/nature11003.
13. **Lin Z, Puetter A, Coco J, Xu G, Strong MJ, Wang X, Fewell C, Baddoo M, Taylor C, Flemington EK.** 2012. Detection of murine leukemia virus in the Epstein-Barr virus-positive human B-cell line JY, using a computational RNA-seq-based exogenous agent detection pipeline, PARSES. J Virol **86:**2970–2977. http://dx.doi.org/10.1128/JVI.06717-11.
14. **Lin Z, Wang X, Strong MJ, Concha M, Baddoo M, Xu G, Baribault C, Fewell C, Hulme W, Hedges D, Taylor CM, Flemington EK.** 2013. Whole-genome sequencing of the Akata and Mutu Epstein-Barr virus strains. J Virol **87:**1172–1182. http://dx.doi.org/10.1128/JVI.02517-12.
15. **Kim DN, Seo MK, Choi H, Kim SY, Shin HJ, Yoon AR, Tao Q, Rha SY, Lee SK.** 2013. Characterization of naturally Epstein-Barr virus-infected gastric carcinoma cell line YCCEL1. J Gen Virol **94:**497–506. http://dx.doi.org/10.1099/vir.0.045237-0.
16. **Ku JL, Kim KH, Choi JS, Kim SH, Shin YK, Chang HJ, Bae JM, Kim YW, Lee JH, Yang HK, Kim WH, Jeong SY, Park JG.** 2012. Establishment and characterization of six human gastric carcinoma cell lines, including one naturally infected with Epstein-Barr virus. Cell Oncol **35:**127–136. http://dx.doi.org/10.1007/s13402-012-0073-9.
17. **Oh ST, Cha JH, Shin DJ, Yoon SK, Lee SK.** 2007. Establishment and characterization of an in vivo model for Epstein-Barr virus positive gastric carcinoma. J Med Virol **79:**1343–1348. http://dx.doi.org/10.1002/jmv.20876.